A strain tensor method for three-dimensional Michell structures

Citation: Jacot, Benjamin P., and Caitlin T. Mueller. "A Strain Tensor Method for Three-Dimensional Michell Structures." Structural and Multidisciplinary Optimization 55, no. 5 (November 29, 2016): 1819–1829.

As Published: http://dx.doi.org/10.1007/s00158-016-1622-z

Publisher: Springer-Verlag

Persistent URL: http://hdl.handle.net/1721.1/109343

Version: Author's final manuscript: final author's manuscript post peer review, without publisher's formatting or copy editing

Structural and Multidisciplinary Optimization manuscript No.
(will be inserted by the editor)

A strain tensor method for three-dimensional Michell structures

Benjamin P. Jacot · Caitlin T. Mueller

Received: date / Accepted: date

Abstract In the design of discrete structures such as trusses and frames, important quantitative goals such as minimal weight or minimal compliance often dominate. Many numerical techniques exist to address these needs. However, an analytical approach exists to meet similar goals, which was initiated by Michell (1904) and has been mostly used for two-dimensional structures so far.

This paper develops a method to extend the existing mainly two-dimensional approach to apply to three-dimensional structures. It will be referred as the Michell strain tensor method (MSTM). First, the proof that MSTM is consistent with the existing theory in two dimensions is provided. Second, two- and three-dimensional known solutions will be replicated based on MSTM. Finally, MSTM will be used to solve new three-dimensional cases.

Keywords Michell structures · Michell wheel · Michell cantilever · Michell sphere · Structural optimization

1 Introduction and background

The seminal paper from Michell (1904) together with theoretical improvements brought by Hemp (1973), Rozvany (1996) and Lewińsky and Sokół (2014) define the mechanical constraints that a structure should respect so as to require the minimal quantity of necessary material. Here, a structure is defined as a finite or infinite set of connected bars which lengths can theoretically be as infinitely small as needed. Also, such bars only work in tension or compression. [1]

More precisely, as first shown in Michell (1904) but also in Hemp (1973), Spillers (1975) or Lewińsky and Sokół (2014), the Principle of Virtual Work applied to a given structure brings:

$$V_t f_t + V_c f_c \geq \frac{W}{\varepsilon} \tag{1}$$

Where:

- V_t and V_c are the total volumes of material of the elements under tension or compression within the structure.
- f_t and f_c are the maximal allowable stresses for tension or compression within the structure.
- W corresponds to the work of external forces.
- ε is the maximal strain within the structure.

The sign of inequality in equation 1 becomes that of equality if:

1. Any member is stressed up to the limit f_t or f_c.
2. Strain is the same in absolute value in every member of the structure.

Such mechanical conditions correspond to Michell's rules. As implicitly shown for the first time in Hemp (1973) and later explicitly by Rozvany (1996, 2014), a structure following Michell's rules is of minimal volume for $f_t = f_c$ only. In such case, the structure can be referred as a Michell structure. If $f_t \neq f_c$, another criteria on strain within the structure is actually derived using Lagrangian optimization on the quantity $V_t + V_c$

B.P. Jacot (✉), C.T. Mueller
Department of Civil and Environmental Engineering,
Massachusetts Institute of Technology,
77 Massachusetts Ave., Cambridge, MA 02139, USA
E-mail: bjacot@mit.edu

[1] This definition relates to truss-like structures. As recently shown in Sigmund et al (2016), other kind of structures, such as plate- or shell-like structures with varying thicknesses, may be more optimal in terms of stiffness or compliance than their truss-like counterparts.

such that the principle of virtual work is verified. Following recommendation given in Rozvany (1996), structures following such criteria should be referred as Hemp structures.

However, most of truss-like structures are built out of steel in the field of civil engineering. In cases where member sizing in tension and compression is governed by permissible stress (and not by buckling), or in those where the design is governed by deflection limits, the tension and compression stresses in a steel structure can be approximated as equal: $f_t = f_c = \sigma$. Therefore, the assumption of equal permissible stresses is made here, which implies that this paper focuses on Michell structures only.

From what precedes it can also be derived that the typical volume V_m of a Michell structure is:

$$V_m = \frac{W}{\sigma\varepsilon} \tag{2}$$

Considering that strains within the structure are implied by the differentiable displacement $\boldsymbol{u}$ that verifies the mechanical hypothesis of small displacements, then by Love (1906):

$$\boldsymbol{\varepsilon} = \frac{1}{2}\left(\boldsymbol{\nabla u} + \boldsymbol{\nabla u}^{\mathsf{T}}\right) \tag{3}$$

Where:

- $\boldsymbol{\nabla u}$ is the gradient matrix associated to $\boldsymbol{u}$.
- $\boldsymbol{\varepsilon}$ is the strain tensor associated to $\boldsymbol{u}$.

Michell's rules apply to $\boldsymbol{\varepsilon}$ as follows[2]:

- For two-dimensional cases, it is shown in Michell (1904) that eigenvalues, or principal strains, of $\boldsymbol{\varepsilon}$ should be equal to ε and $-\varepsilon$, where ε is a non-zero constant parameter. Also, elements of the structure should follow the orientations of the lines of principal strain of $\boldsymbol{\varepsilon}$.
- For three-dimensional cases, it is shown in Lewińsky and Sokół (2014) that the maximal and minimal principal strains of $\boldsymbol{\varepsilon}$ should be equal to ε and $-\varepsilon$, where ε is again a non-zero constant parameter. Also, elements of the structure should follow the orientations of the lines of maximal and minimal principal strains.

For a long time, three-dimensional Michell structures were thought to have constraints on their intermediate principal strain, as in Ghista and Resnikoff (1968) or Hemp (1973): the latter was thought to be equal to either ε and $-\varepsilon$. It actually turns out not to be necessary, according to Lewińsky (2004) and Lewińsky and Sokół (2014): the intermediate strain is free to vary between ε and $-\varepsilon$. In this paper for example, case studies for three-dimensional structures have a zero-valued intermediate strain.

[2] These rules, and MSTM by derivation, are valid in T-regions only, defined in Sokół and Rozvany (2012) or Lewińsky and Sokół (2014) as regions where Michell structures have orthogonal tension and compression elements.

2 Theory and methodology

2.1 Principles of MSTM

The key idea for the new Michell Strain Tensor Method is that information on $\boldsymbol{u}$ simplifies the calculation of $\boldsymbol{\varepsilon}$ in equation 3. If such information is correct, then $\boldsymbol{\varepsilon}$ should fit to the geometry of the problem, respect the boundary conditions and follow Michell's rules. $\boldsymbol{\varepsilon}$ being analytically determined, the corresponding Michell structure can be drawn by following the lines of principal strains of $\boldsymbol{\varepsilon}$.

2.2 Proof of equivalence between MSTM in 2D and Hemp & Chan procedure

The development of Michell structures follows a procedure developed in Chan (1960) and Hemp (1973) for two-dimensional cases. Because of its major role in the development of Michell structures, it is necessary to prove that MSTM is equivalent to this previously developed procedure. This is the focus of this section of the paper.

First, S is defined as a 2D orthogonal curvilinear coordinate system whose variables are (α, β) and basis vectors are $(\boldsymbol{e_\alpha}, \boldsymbol{e_\beta})$. Ω is the region of plane in which Michell structures are allowed to exist.

In either Chan (1960), equation 10, or Hemp (1973), equation 4.22, Michell structures are generated based on an angular potential ϕ, solution of:

$$\frac{\phi}{\alpha}\beta = 0 \tag{4}$$

Equation 4 is explicitely recognized as the characterization of Michell structures in Chan (1960), Hemp (1973) or Strang and Kohn (1983). The intent of this proof is hence to show that the logical steps leading to equation 4 are similar to those used in the definition of MSTM.

Following Sadd (2005), section 1.9, basis vectors of S are such that:

$$\begin{aligned}
\frac{\boldsymbol{e_\alpha}}{\alpha} &= -\frac{1}{B}\frac{A}{\beta}\boldsymbol{e_\beta}, \quad \frac{\boldsymbol{e_\alpha}}{\beta} = \frac{1}{A}\frac{B}{\alpha}\boldsymbol{e_\beta} \\
\frac{\boldsymbol{e_\beta}}{\beta} &= -\frac{1}{A}\frac{B}{\alpha}\boldsymbol{e_\alpha}, \quad \frac{\boldsymbol{e_\beta}}{\alpha} = \frac{1}{B}\frac{A}{\beta}\boldsymbol{e_\alpha}
\end{aligned} \tag{5}$$

Where A and B are the scale factors of S in the respective directions $\boldsymbol{e_\alpha}$ and $\boldsymbol{e_\beta}$ and are functions of the plane coordinates. Also, $\boldsymbol{u}$ is expressed in S as:

$$\boldsymbol{u} = u_\alpha \boldsymbol{e_\alpha} + u_\beta \boldsymbol{e_\beta} \tag{6}$$

Equations 5 and 6 bring:

$$\boldsymbol{\nabla u} = \begin{pmatrix} \frac{1}{A}\frac{\partial u_\alpha}{\partial \alpha} + \frac{1}{AB}\frac{\partial A}{\partial \beta}u_\beta & \frac{1}{B}\frac{\partial u_\alpha}{\partial \beta} - \frac{1}{AB}\frac{\partial B}{\partial \alpha}u_\beta \\ \frac{1}{A}\frac{\partial u_\beta}{\partial \alpha} - \frac{1}{AB}\frac{\partial A}{\partial \beta}u_\alpha & \frac{1}{B}\frac{\partial u_\beta}{\partial \beta} + \frac{1}{AB}\frac{\partial B}{\partial \alpha}u_\alpha \end{pmatrix} \tag{7}$$

Also:

$$\frac{1}{A}\frac{\partial u_\beta}{\partial \alpha} - \frac{1}{AB}\frac{\partial B}{\partial \alpha}u_\beta + \frac{1}{B}\frac{\partial u_\alpha}{\partial \beta} - \frac{1}{AB}\frac{\partial A}{\partial \beta}u_\alpha = \frac{B}{A}\frac{\partial}{\partial \alpha}\frac{u_\beta}{B} + \frac{A}{B}\frac{\partial}{\partial \beta}\frac{u_\alpha}{A} \tag{8}$$

Using equations 3, 7 and 8, the strain tensor is:

$$\boldsymbol{\varepsilon} = \begin{pmatrix} \frac{1}{A}\frac{\partial u_\alpha}{\partial \alpha} + \frac{1}{AB}\frac{\partial A}{\partial \beta}u_\beta & \frac{B}{2A}\frac{\partial}{\partial \alpha}\frac{u_\beta}{B} + \frac{A}{2B}\frac{\partial}{\partial \beta}\frac{u_\alpha}{A} \\ \frac{B}{2A}\frac{\partial}{\partial \alpha}\frac{u_\beta}{B} + \frac{A}{2B}\frac{\partial}{\partial \beta}\frac{u_\alpha}{A} & \frac{1}{B}\frac{\partial u_\beta}{\partial \beta} + \frac{1}{AB}\frac{\partial B}{\partial \alpha}u_\alpha \end{pmatrix} \tag{9}$$

From here, Hemp-Chan procedure differs from MSTM and each needs to be studied separately.

Michell strain tensor method In MSTM, equation 9 may or may not express $\boldsymbol{\varepsilon}$ in the basis in which the latter is diagonal. What only matters is whether $\boldsymbol{\varepsilon}$ is such that it meets Michell's rules. It means that the principal strains of $\boldsymbol{\varepsilon}$ shall be equal in absolute value and opposed in sign, which forces the trace of $\boldsymbol{\varepsilon}$ to be zero-valued. $\boldsymbol{\varepsilon}$ becomes:

$$\boldsymbol{\varepsilon} = \begin{pmatrix} \varepsilon_\alpha & \varepsilon_{\alpha\beta} \\ \varepsilon_{\alpha\beta} & -\varepsilon_\alpha \end{pmatrix} \tag{10}$$

With:

$$\begin{aligned} \varepsilon_\alpha &= \frac{1}{A}\frac{\partial u_\alpha}{\partial \alpha} + \frac{1}{AB}\frac{\partial A}{\partial \beta}u_\beta = -\left(\frac{1}{B}\frac{\partial u_\beta}{\partial \beta} + \frac{1}{AB}\frac{\partial B}{\partial \alpha}u_\alpha\right) \\ \varepsilon_{\alpha\beta} &= \frac{B}{2A}\frac{\partial}{\partial \alpha}\frac{u_\beta}{B} + \frac{A}{2B}\frac{\partial}{\partial \beta}\frac{u_\alpha}{A} \end{aligned} \tag{11}$$

Michell's rules stating that eigenvalues ε_{I} and $\varepsilon_{\mathrm{II}}$ of $\boldsymbol{\varepsilon}$ should be equal in absolute value to ε and opposed in sign, it follows that:

$$\varepsilon_{\mathrm{I}} = \sqrt{\varepsilon_\alpha^2 + \varepsilon_{\alpha\beta}^2} = \varepsilon, \quad \varepsilon_{\mathrm{II}} = -\varepsilon_{\mathrm{I}} \tag{12}$$

If a solution to the above equation is found, then $\boldsymbol{\varepsilon}$ is acceptable, as it meets Michell's rules. Eigenvectors $\boldsymbol{\pi}_{\mathrm{I}}$ and $\boldsymbol{\pi}_{\mathrm{II}}$ of $\boldsymbol{\varepsilon}$ can be computed on every point within Ω so as to generate the corresponding Michell structure.

Hemp-Chan procedure In Hemp-Chan procedure, equation 9 must express $\boldsymbol{\varepsilon}$ in the basis in which the latter is diagonal. Equation 12 is therefore not directly solved - whereas it is in MSTM.

Instead, Hemp-Chan procedure introduces the angle ϕ that $\boldsymbol{e_\alpha}$ shares with a fixed vector of the Cartesian coordinate system, say $\boldsymbol{e_x}$. ϕ is such that the tensor $\boldsymbol{\varepsilon}$ is in its diagonal form:

$$\boldsymbol{\varepsilon} = \begin{pmatrix} \varepsilon & 0 \\ 0 & -\varepsilon \end{pmatrix} \tag{13}$$

In other words, ϕ is the rotation for the Cartesian basis vectors to become the diagonalizing basis of the strain tensor at point M(α,β). From the definition of ϕ it follows that:

$$\begin{aligned} \boldsymbol{e_\alpha} &= \cos(\phi)\boldsymbol{e_x} + \sin(\phi)\boldsymbol{e_y} \\ \boldsymbol{e_\beta} &= -\sin(\phi)\boldsymbol{e_x} + \cos(\phi)\boldsymbol{e_y} \end{aligned} \tag{14}$$

Derivatives of $\boldsymbol{e_\alpha}$ are then:

$$\begin{aligned} \frac{\boldsymbol{e_\alpha}}{\alpha} &= \frac{\phi}{\alpha}\left(-\sin(\phi)\boldsymbol{e_x} + \cos(\phi)\boldsymbol{e_y}\right) = \frac{\phi}{\alpha}\boldsymbol{e_\beta} \\ \frac{\boldsymbol{e_\alpha}}{\beta} &= \frac{\phi}{\beta}\left(-\sin(\phi)\boldsymbol{e_x} + \cos(\phi)\boldsymbol{e_y}\right) = \frac{\phi}{\beta}\boldsymbol{e_\beta} \end{aligned} \tag{15}$$

Comparing equations 5 and 15 brings:

$$\frac{\phi}{\alpha} = -\frac{1}{B}\frac{A}{\beta}, \quad \frac{\phi}{\beta} = \frac{1}{A}\frac{B}{\alpha} \tag{16}$$

which corresponds to equation 4.14 in Hemp (1973) or 6 in Chan (1960). Then, the solution for ϕ can be found by equaling equations 9 and 13, while taking equation 16 into account. Result is:

$$\begin{aligned} &\frac{1}{A}\left(\frac{\partial u_\alpha}{\partial \alpha} - \frac{\partial \phi}{\partial \alpha}u_\beta\right) = \varepsilon \\ &\frac{1}{B}\left(\frac{\partial u_\beta}{\partial \beta} + \frac{\partial \phi}{\partial \beta}u_\alpha\right) = -\varepsilon \\ &\frac{1}{A}\left(\frac{\partial u_\beta}{\partial \alpha} + \frac{\partial \phi}{\partial \alpha}u_\alpha\right) + \frac{1}{B}\left(\frac{\partial u_\alpha}{\partial \beta} - \frac{\partial \phi}{\partial \beta}u_\beta\right) = 0 \end{aligned} \tag{17}$$

Introducing the local rotation ω as defined in Love (1906), equation 38 and used in Chan (1960) will make the rest of the calculation more straightforward. This is the only reason why it is introduced, as there is no condition on ω. By definition:

$$2\omega = \frac{1}{AB}\left(\frac{B}{\alpha}u_\beta - \frac{A}{\beta}u_\alpha\right) + \frac{1}{A}\frac{u_\beta}{\alpha} - \frac{1}{B}\frac{u_\alpha}{\beta} \tag{18}$$

And, by taking equation 16 into account:

$$2\omega = \frac{1}{A}\left(\frac{u_\beta}{\alpha} + \frac{\phi}{\alpha}u_\alpha\right) - \frac{1}{B}\left(\frac{u_\alpha}{\beta} - \frac{\phi}{\beta}u_\beta\right) \tag{19}$$

Combining equations 17 and 19 returns:

$$\begin{aligned} \frac{\partial u_\alpha}{\partial \alpha} &= A\varepsilon + \frac{\partial \phi}{\partial \alpha}u_\beta, \quad \frac{\partial u_\alpha}{\partial \beta} = -B\omega + \frac{\partial \phi}{\partial \beta}u_\beta \\ \frac{\partial u_\beta}{\partial \beta} &= -B\varepsilon - \frac{\partial \phi}{\partial \beta}u_\alpha, \quad \frac{\partial u_\beta}{\partial \alpha} = A\omega - \frac{\partial \phi}{\partial \alpha}u_\alpha \end{aligned} \tag{20}$$

As in Chan (1960), elimination of u_α and u_β within the above set of equations gives:

$$\frac{\partial}{\partial \alpha}(\omega - 2\varepsilon\phi) = 0, \quad \frac{\partial}{\partial \beta}(\omega + 2\varepsilon\phi) = 0 \tag{21}$$

ε being a constant, the elimination of ω in equation 21 brings that ϕ verifies equation 4.

Proof conclusion The analysis of the Hemp-Chan procedure has shown that Michell structures were generated by finding the curvilinear basis at point M (α,β) in which the strain tensor $\boldsymbol{\varepsilon}$ is diagonal and follows Michell's rules. The aforementioned curvilinear basis is parametrized by the angle ϕ it has with the Cartesian basis. All these conditions lead to solving the equations shown in equation 17, which turns out to be equivalent to solving equation 4.

In MSTM, the curvilinear basis remains constant. The strain tensor $\boldsymbol{\varepsilon}$ is expressed in such basis and implemented to see if it can satisfy Michell's rules. If it does, eigenvectors of $\boldsymbol{\varepsilon}$ are computed and the Michell structure is generated. Therefore, the curvilinear basis at point M (α,β) in which the strain tensor $\boldsymbol{\varepsilon}$ is diagonal is found after ensuring that $\boldsymbol{\varepsilon}$ respects Michell's rules, and not at the same time as in Hemp-Chan procedure. Note that diagonalizing $\boldsymbol{\varepsilon}$ is not about rotating the Cartesian basis anymore, but the curvilinear basis of reference.

By showing that the only true difference between Hemp-Chan procedure and MSTM is about when the diagonalization of $\boldsymbol{\varepsilon}$ is performed and what the affected basis is, we conclude that both methods are equivalent in 2D. Ultimately, both methods find the exact same basis in which $\boldsymbol{\varepsilon}$ is diagonal, and use its basis vectors to generate a Michell structure.

Both methods are equivalent in 2D, but MSTM has advantages in 3D over Hemp-Chan procedure. In 3D, the latter would indeed require the introduction of two other angles in equation 14, each referring to the rotation to perform around each of the three axes. Equations within the Hemp-Chan procedure would therefore incorporate additional terms and become much more difficult to solve. Also, if the use of complex variables in Hemp (1973), chapter 4, makes Hemp-Chan procedure work simply and elegantly in 2D, it can't be extended to 3D. Complex variables are indeed powerful objects to simplify the analysis of 2D problems only, by integrating one direction of the plane in their real part and the other in their imaginary part.

In contrast, MSTM can easily apply to 3D by using a 3×3 tensor matrix rather than a 2×2 one, with no change in any equation required. Indeed, algebraic operations on tensor matrices work the same whatever the dimension of a square matrix may be. This is what fundamentally makes MSTM a suitable method to investigate Michell structures in 3D.

3 MSTM algorithm

In this section, the algorithm corresponding to MSTM is defined. It is designed to draw lines which are part of a Michell structure and works for either two or three dimensional cases. The functioning is as follows:

- Step 0 (pre-initialization). Ω is defined and $\boldsymbol{\varepsilon}$ is determined to meet the boundary conditions of the problem and be solution of equation 12. A step value δ used in step 4 is also defined at this stage.
- Step 1: A set of starting points $\left(M_{0,i}\right)_{1\leq i\leq K}$ is selected, preferably on a border of Ω.
- Step 2: $\boldsymbol{\varepsilon}$ is estimated for each $M_{0,i}$.
- Step 3: Eigenvectors $\boldsymbol{\pi}_{\mathrm{I},\boldsymbol{i}}$ and $\boldsymbol{\pi}_{\mathrm{II},\boldsymbol{i}}$ of $\boldsymbol{\varepsilon}$ are computed for each $M_{0,i}$. $\boldsymbol{\pi}_{\mathrm{I},\boldsymbol{i}}$ and $\boldsymbol{\pi}_{\mathrm{II},\boldsymbol{i}}$ correspond to the respective maximal and minimal eigenvalue of $\boldsymbol{\varepsilon}$, $+\varepsilon$ and -ε, $\varepsilon > 0$.
- Step 4: $M_{1,i}$ and $M_{2,i}$ are defined to have a first order approximation of the Michell structure:

  $$\boldsymbol{OM_{1,i}} = \boldsymbol{OM_{0,i}} + \delta\boldsymbol{\pi}_{\mathrm{I},\boldsymbol{i}}, \quad \boldsymbol{OM_{2,i}} = \boldsymbol{OM_{0,i}} + \delta\boldsymbol{\pi}_{\mathrm{II},\boldsymbol{i}}$$

  Where O is the origin of the coordinate system and δ the precision by which one wishes to discretize the curved lines of the structure. It is enough for δ to be an order of magnitude or two less than the typical dimensions of Ω for the resulting structure to be smooth enough.
- Step 5: Members $[M_{0,i}M_{1,i}]$ and $[M_{0,i}M_{2,i}]$ are drawn.
- Step 6: $\boldsymbol{\varepsilon}$ is estimated for each $M_{1,i}$ and $M_{2,i}$.
- Step 7: $\boldsymbol{\pi}_{\mathrm{I},\boldsymbol{i}}$ is computed for each $M_{1,i}$ and $\boldsymbol{\pi}_{\mathrm{II},\boldsymbol{i}}$ for each $M_{2,i}$.

– Step 8: $M'_{1,i}$ and $M'_{2,i}$ are defined as:

$$\boldsymbol{OM'_{1,i}} = \boldsymbol{OM_{1,i}} + \delta\boldsymbol{\pi}_{\mathrm{I},\boldsymbol{i}}, \quad \boldsymbol{OM'_{2,i}} = \boldsymbol{OM_{2,i}} + \delta\boldsymbol{\pi}_{\mathrm{II},\boldsymbol{i}}$$

– Step 9: Members $[M_{1,i}M'_{1,i}]$ and $[M_{2,i}M'_{2,i}]$ are drawn.
– Step 10: $M_{1,i} \leftarrow M'_{1,i}$ and $M_{2,i} \leftarrow M'_{2,i}$ and go back to step 6 as long as $M_{1,i}$ and $M_{2,i}$ are within Ω.

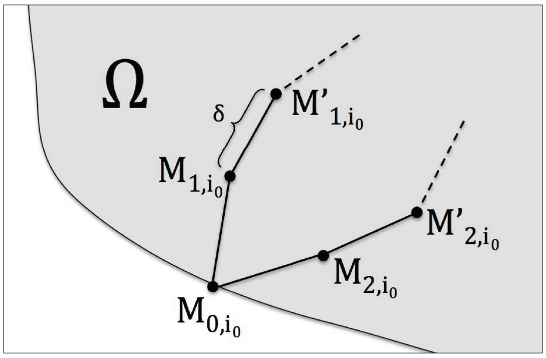

Fig. 1: Functioning of the tensor-based algorithm.

Figure 1 illustrates the typical functioning of the algorithm for a given i. Steps 6 to 10 make the complexity of the algorithm equal to $\mathcal{O}(1)$, which implies fast computation time. The algorithm hence generates the lines of principal strains corresponding to tension or compression starting at $\left(M_{0,i}\right)_{1\leq i\leq K}$ and reaching a boundary of Ω. As optimum structures typically consist in an infinite amount of tension and compression lines, the algorithm only generates sub-sets of such structures.

4 Results in 2D

4.1 Case study: Michell wheel

ing

$V_m = 2$ … σ

There has no … Michell wheel so… the volume of Mich…

4.2 Case study: Michell can…

Problem statement From previou… ber of nodes at the external bound… equal to 1. Hence, structures are no… a local orthoradial loading $\boldsymbol{F_\theta}$ … located at $r = R_2$ - see figure…

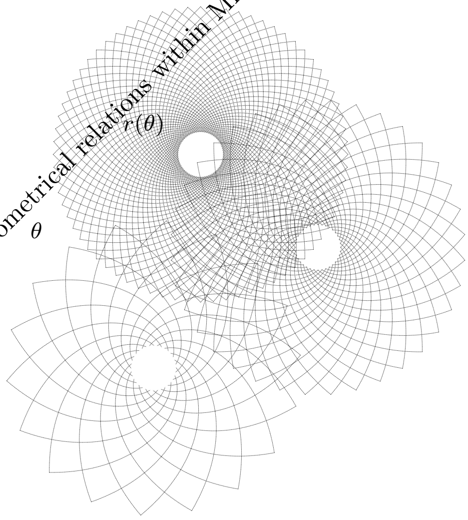

Fig. 3: Geometrical relations within Michell wheel.

Fig. 4: MSTM output - 18 (top left), 36 (bottom center) and 72 (top right) starting points.

MSTM generation of solutions The results obtained from MSTM algorithm correspond to the expectati… from the previous subsection. They are shown in… 4 for different values of starting points on the… $r = R_2$ of Ω. The algorithm terminates on…

Equation of the Michell wheel lines … it can be derived that:

$$r\frac{\mathrm{d}\theta}{\mathrm{d}r} = \tan\left(\pm\frac{\pi}{4}\right) = \pm 1$$

This leads to:

$$r(\theta) = \pm R_1 e^{(\theta-\theta_0)}$$ …

Such equati… R_1. Agai… (1973)…

MSTM generation of solutions The starting point of the algorithm corresponds to the location of the point load and results are shown in figure 6. Such structures correspond to the solution found in Michell (1904), as reproduced in figure 7.

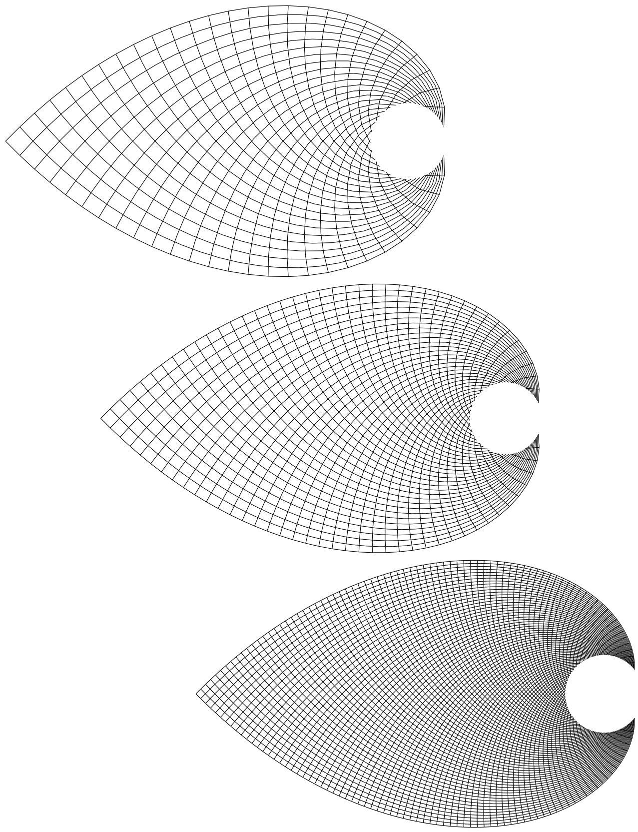

Fig. 6: Cantilever solution for decreasing values of the step parameter δ.

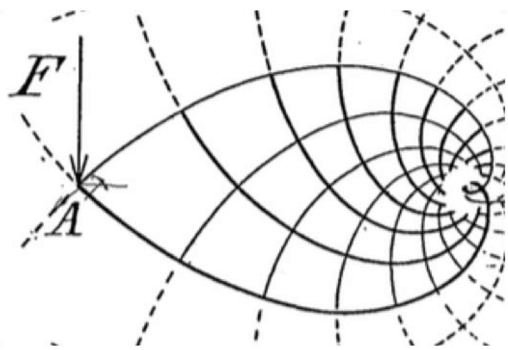

Fig. 7: Original Michell (1904) cantilever.

5 Results in 3D

Spherical coordinates (r,φ,θ) are used, as defined in Sadd (2005). It follows that: $r \in \mathbb{R}^+, \theta \in [0, 2\pi), \varphi \in [0, \pi]$. θ is the radial angle, φ is the colatitude angle.

5.1 Case study: Michell sphere

Finding the strain tensor From equations 3 and 36 it can be shown that:

$$\boldsymbol{\varepsilon} = \varepsilon_{\varphi\theta}(\varphi)\boldsymbol{M_{\varphi\theta}} \tag{39}$$

Where:

$$\varepsilon_{\varphi\theta}(\varphi) = \frac{\sin(\varphi)}{2}\frac{\mathrm{d}\omega}{\mathrm{d}\varphi}, \quad \boldsymbol{M_{\varphi\theta}} = \begin{pmatrix} 0 & 0 & 0 \\ 0 & 0 & 1 \\ 0 & 1 & 0 \end{pmatrix} \tag{40}$$

For this 3D case, equation 12 becomes:

$$\sin(\varphi)\frac{\mathrm{d}\omega}{\mathrm{d}\varphi} = 2\varepsilon \tag{41}$$

And solutions exist for $0 < \varphi_1 \leq \varphi < \pi$. Taking the first boundary condition in equation 38 into account, integration of equation 41 is:

$$\omega(\varphi) - \omega_1 = 2\varepsilon \ln\left(\frac{\tan(\varphi/2)}{\tan(\varphi_1/2)}\right) \tag{42}$$

In order to satisfy the second boundary condition in equation 38, a condition on the parameter ε arises (mathematically true for $\varphi_1 \neq \varphi_2$, which is always the case):

$$\varepsilon = \frac{\omega_2 - \omega_1}{2}\left[\ln\left(\frac{\tan(\varphi_2/2)}{\tan(\varphi_1/2)}\right)\right]^{-1} \tag{43}$$

Which gives:

$$\omega(\varphi) = (\omega_2 - \omega_1)\frac{\ln(\tan(\varphi/2)) - \ln(\tan(\varphi_1/2))}{\ln(\tan(\varphi_2/2)) - \ln(\tan(\varphi_1/2))} + \omega_1 \tag{44}$$

Hence an expression for $\boldsymbol{\varepsilon}$ has been found so as to apply to Michell's rules and to the boundary conditions:

$$\boldsymbol{\varepsilon} = \frac{\omega_2 - \omega_1}{2}\left[\ln\left(\frac{\tan(\varphi_2/2)}{\tan(\varphi_1/2)}\right)\right]^{-1}\boldsymbol{M_{\varphi\theta}} \tag{45}$$

MSTM generation of solutions The two maximum and minimum eigenvectors $\boldsymbol{\pi}_{\mathrm{I}}$ and $\boldsymbol{\pi}_{\mathrm{III}}$ found from equation 45 have the following directions:

$$\boldsymbol{\pi}_{\mathrm{I}} \parallel \boldsymbol{e_\theta} + \boldsymbol{e_\varphi}, \quad \boldsymbol{\pi}_{\mathrm{III}} \parallel \boldsymbol{e_\theta} - \boldsymbol{e_\varphi} \tag{46}$$

Relying on the algorithm introduced in section 3, solutions have been generated. Accuracy has been increased by adding more starting points on the disc perimeter on $\varphi = \varphi_1$ - keeping all other parameters R, R_1 and R_2 equal. Also, MSTM algorithm terminates once $\varphi \geq \varphi_2$. Such a generation is shown in figure 9a. Figure 9b shows how solutions vary with R_1 and R_2.

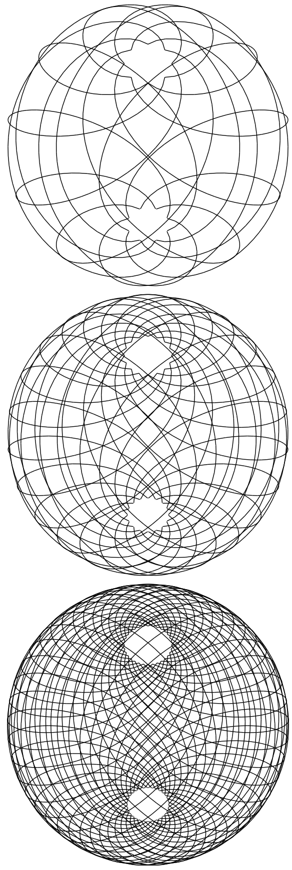

(a) 8, 16 and 32 starting points.

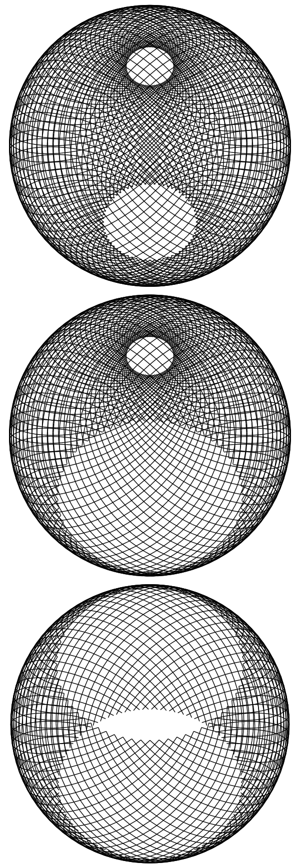

(b) Different disc radii R_1 and R_2.

Fig. 9: Parametrized solutions.

Equation of the Michell sphere lines An infinitely small displacement $\mathrm{d}\boldsymbol{OM}$ is expressed in spherical coordinates as:

$$\mathrm{d}\boldsymbol{OM} = \mathrm{d}r\boldsymbol{e_r} + r\sin(\varphi)\,\mathrm{d}\theta\boldsymbol{e_\theta} + r\,\mathrm{d}\varphi\boldsymbol{e_\varphi} \tag{47}$$

In addition, $\mathrm{d}\boldsymbol{OM} \parallel \boldsymbol{\pi}_{\mathrm{I}}$ *or* $\boldsymbol{\pi}_{\mathrm{III}}$. Hence:

$$\mathrm{d}r = 0, \quad r\sin(\varphi)\,\mathrm{d}\theta = \pm r\,\mathrm{d}\varphi \tag{48}$$

Finding $\mathrm{d}r = 0$ explicitly shows that the lines of the structure will remain on a same sphere. The Michell structure is therefore a surface, or shell, as proved in Lewińsky and Sokół (2014) for the general case. A solution for the second part of equation 48 with $\varphi_0 > 0$ and $\varphi < \pi$ is:

$$\theta(\varphi) - \theta(\varphi_0) = \pm\ln\left(\frac{\tan(\varphi/2)}{\tan(\varphi_0/2)}\right) \tag{49}$$

The above equation defines a typical line part of the torque-resisting structure, plotted in figure 10.

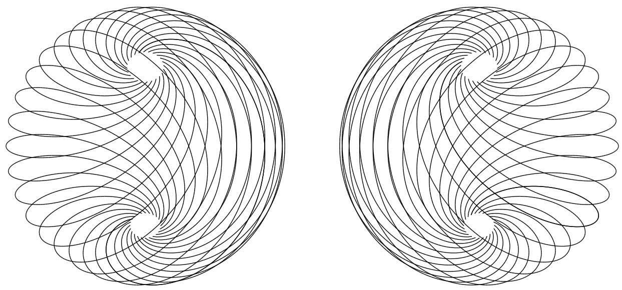

Fig. 10: The two sets of lines from equation 49 - compression or tension.

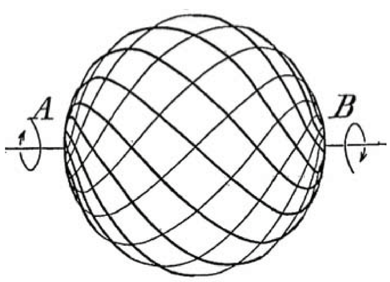

Fig. 11: The original sphere, as shown in Michell (1904).

Volume of Michell sphere As described in 5.1 *Problem statement*, the motion of the two discs is caused by torques - namely, $-T$ and T on discs of respective radius R_1 and R_2 for external equilibrium to be maintained. The work of external forces W is:

$$W = T(\omega_2 - \omega_1) \tag{50}$$

Applying equations 45 and 50 in equation 2, the volume V_m of the Michell sphere is:

$$V_m = \frac{2T}{\sigma} \ln\left(\frac{\tan(\varphi_2/2)}{\tan(\varphi_1/2)}\right) \tag{51}$$

which is identical to Lewińsky (2004), equation 76. The simplified case in Michell (1904) shown in figure 11 applies for:

$$\begin{aligned} &R_1 = R_2, \quad \omega_2 = -\omega_1 = \omega \\ &p_{2,\theta} = -p_{1,\theta} = p_\theta, \quad \varphi_2 = \pi - \varphi_1 \end{aligned} \tag{52}$$

Here equation 51 reduces to:

$$V_m = \frac{4T}{\sigma} \ln\Big(\cot\left(\varphi_1/2\right)\Big) \tag{53}$$

This equation is identical to Hemp (1973), equation 4.100 and Lewińsky (2004), equation 77 for the same case.

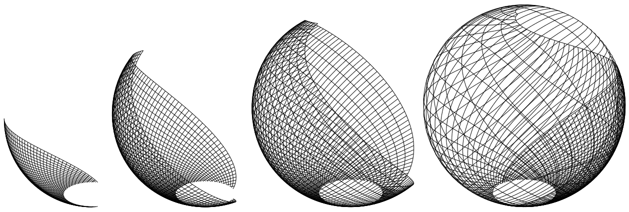

Fig. 13: Evolution of the cantilever solution. From left to right: $\frac{R_1}{R_2} = 3$, 2, 1 and 0.2.

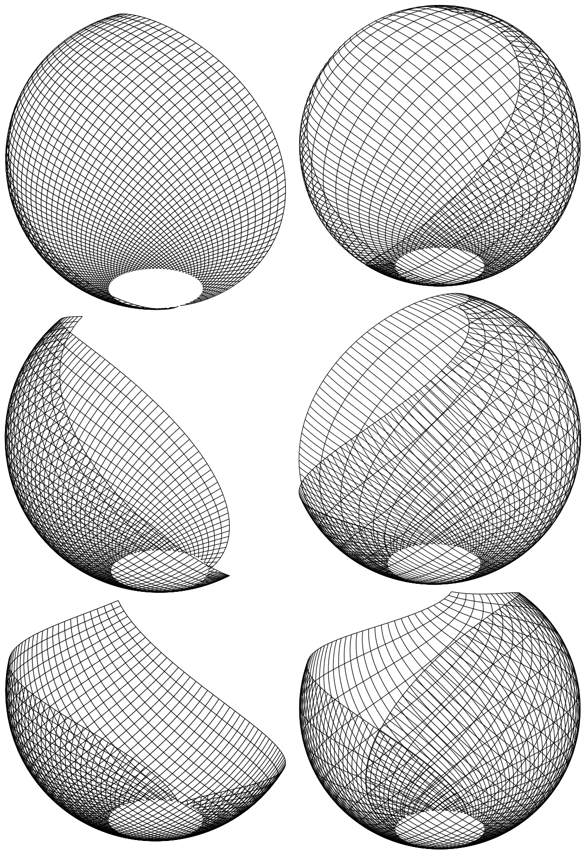

(a) Case $R_1 > R_2$. (b) Case $R_1 < R_2$.

Fig. 14: Views of typical 3D Michell cantilever solutions.

5.3 Case study: Spinning spheres

Problem statement This problem has, to date, not been studied. Two concentric spinning spheres S_1 and S_2 are defined, with respective radii R_1 and R_2, such that $R_1 < R_2$. Their common center is O. Ω is the region of space between the two spheres.

Angular displacements ω_1 and ω_2 on each sphere are constant. Therefore, each sphere rotates in an uniform way. As both the geometry and the motion conditions of the problem are invariant with respects to θ, θ is not a variable for any function describing the problem.

of the equation, 2ε. Therefore both (α) $r\dfrac{\mathrm{d}\omega}{\mathrm{d}r}$ and (β) $\sin(\varphi)$ shall be constant.

Condition (β) implies that if a Michell structure exists, it will necessarily have every members lying on two cones of equation $\varphi = \varphi_0$ and $\varphi = \pi - \varphi_0$, with $\varphi_0 \in \; (0, \frac{\pi}{2}]$, such that $\sin(\varphi)$ is a constant. A typical solution for the spinning spheres problem will therefore be a set of Michell cones.

Also, solving condition (α) is equivalent to solving equation 63 adapted to condition (β):

$$r\frac{\mathrm{d}\omega}{\mathrm{d}r} = \frac{2\varepsilon}{\sin(\varphi_0)} \tag{64}$$

A solution that meets the first boundary condition in equation 57 is:

$$\omega(r) = \frac{2\varepsilon}{\sin(\varphi_0)} \ln\left(\frac{r}{R_1}\right) + \omega_1 \tag{65}$$

And the second boundary condition is met for:

$$\varepsilon = \sin(\varphi_0)\frac{\omega_2 - \omega_1}{2}\left(\ln\left(\frac{R_2}{R_1}\right)\right)^{-1} \tag{66}$$

Hence, a family of Michell structures has been found, parametrized by φ_0. If all structures have constant maximal and minimal principal strains which are equal in absolute value and opposed, they may not all be of minimal volume though.

More precisely, equation 66 shows that the principal strains vary with φ_0: $\varepsilon_{\mathrm{I}} = -\varepsilon_{\mathrm{III}} = \varepsilon(\varphi_0)$. The volume for each Michell structure, as defined in equation 2, will therefore vary with φ_0 as well - see equation 69.

In view of what precedes, the strain tensor $\boldsymbol{\varepsilon}$ is:

$$\boldsymbol{\varepsilon} = \sin(\varphi_0)\frac{\omega_2 - \omega_1}{2}\left(\ln\left(\frac{R_2}{R_1}\right)\right)^{-1} \boldsymbol{M_{r\theta}} \tag{67}$$

Volume of the Michell cones For a torque T on $R = R_2$, external equilibrium brings that the torque on $R = R_1$ is $-T$. The work of external forces is:

$$W = T(\omega_2 - \omega_1) \tag{68}$$

Combining equations 2, 66 and 68, the volume of a Michell structure is:

$$V_m = \frac{2T}{\sigma \sin(\varphi_0)} \ln\left(\frac{R_2}{R_1}\right) \tag{69}$$

The absolute minimal structure is found for $\varphi_0 = \frac{\pi}{2}$, which corresponds to the 2D Michell wheel - as shown in equation 33. Interestingly enough, this two-dimensional Michell structure is the optimal solution for the three-dimensional case under consideration - which would have been challenging to intuit.

Michell structures on cones $\varphi = \varphi_0$ and $\varphi = \pi - \varphi_0$ are not the optimal solution within Ω, but they are within $\Omega \cap D$, where D is the region of space in which φ is such that $|\pi/2 - \varphi_0| \leq |\pi/2 - \varphi|$. In such domain, Michell cantilevers can also be derived from Michell cones the same way they have been derived from Michell sphere. Such structures won't be as economical though, because they are constrained to exist in a reduced portion of space, i.e. Ω is smaller.

MSTM generation of solutions Figure 16 shows the family of Michell structures and their corresponding volume-based performance scores $\gamma(\varphi_0)$, with:

$$\gamma(\varphi_0) = \frac{V_m(\varphi_0)}{V_m(\pi/2)} = \frac{1}{\sin(\varphi_0)} \tag{70}$$

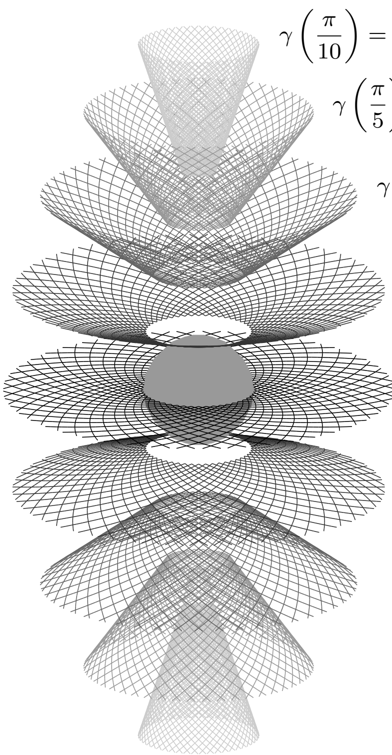

Fig. 16: Different Michell structures. The darker the structure, the more economically efficient.

Equation of the Michell cones lines From equation 67, eigenvectors $\boldsymbol{\pi}_{\mathrm{I}}$ and $\boldsymbol{\pi}_{\mathrm{III}}$ of $\boldsymbol{\varepsilon}$ are such that:

$$\boldsymbol{\pi}_{\mathrm{I}} \parallel \boldsymbol{e_r} + \boldsymbol{e_\theta}, \quad \boldsymbol{\pi}_{\mathrm{III}} \parallel \boldsymbol{e_r} - \boldsymbol{e_\theta} \tag{71}$$

By equation 47, it leads to solving:

$$r\,\mathrm{d}\varphi = 0, \quad \mathrm{d}r = \pm r\sin(\varphi)\,\mathrm{d}\theta \tag{72}$$

As $r > 0$, $\mathrm{d}\varphi = 0$ and members stay on conical surfaces $\varphi = \varphi_0$. Solutions for equation 72 are plotted in figure 17 and have the following expression:

$$r(\theta) = R_1 e^{\pm \sin(\varphi_0)(\theta - \theta_0)} \tag{73}$$

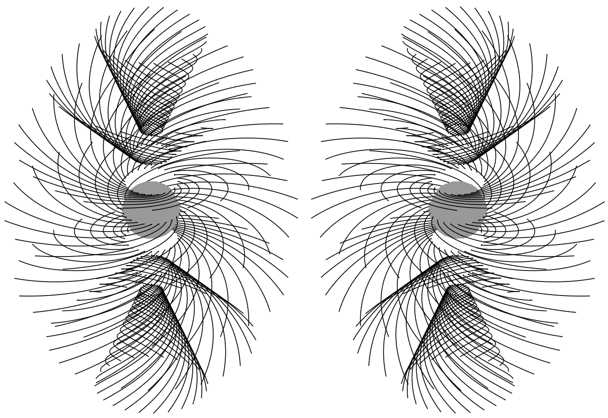

Fig. 17: The two sets of lines from equation 73 - compression or tension.

6 Conclusion

A new analytical method for finding Michell structures has been defined in this paper: the Michell strain tensor method, or MSTM. The latter has been proved equivalent to the existing mathematical methods of Chan (1960) and Hemp (1973). It has also been implemented on known two-dimensional cases to ensure results from MSTM were consistent with existing studies.

Nevertheless, the paper has also shown that MSTM has the advantage of easier applications to three-dimensional problems. MSTM relies on strain tensors which can describe either two- or three-dimensional problems through 2×2 or 3×3 matrices. In contrast, equation 4 from Chan (1960) and Hemp (1973) does not hold true in three dimensions, because it does not take the additional direction of space into account.

MSTM paves the way for new three-dimensional Michell structures to be found, hence enabling the transfer of loads from one location in space to another in the most economical way possible. The case studies from this paper are analytically solvable mostly because their geometrical characteristics fit well with the polar and spherical coordinate systems under consideration. In the future, other three-dimensional case studies can be investigated for other coordinate systems.

Furthermore, the ideas presented in this paper may be explored and extended through numerical methods, possibly leading to the discovery of additional new optimal structures. For such methods, the main challenge to address is the computation of a displacement field $\boldsymbol{u}$ that meets Michell's rules.

References

Chan ASL (1960) The design of Michell optimum structures. Aeronautical Research Council Reports and Memoranda 3303

Ghista DN, Resnikoff MM (1968) Development of Michell minimum weight structures. NASA Technical Notes D-4345

Hemp WS (1973) Optimum structures, Oxford university press, chap 4, pp 70–101. Oxford Engineering Science Series

Lewińsky T (2004) Michell structures formed on surfaces of revolution. Structural and Multidisciplinary Optimization 28:20–30, doi:10.1007/s00158-004-0419-7

Lewińsky T, Sokół T (2014) On basic properties of Michell's structures. Topology Optimization in Structural and Continuum Mechanics 549:87–128, doi:10.1007/978-3-7091-1643-2_6

Love AEH (1906) A treatise on the mathematical theory of elasticity, 2nd edn. Cambridge University Press

Michell AGM (1904) The limit of economy of material in frame structures. PhilMag Series VI 8

Rozvany GIN (1996) Some shortcomings in Michell's truss theory. Structural and Multidisciplinary Optimization 12:244–250, doi:10.1007/BF01197364

Rozvany GIN (2014) Structural topology optimization (sto) - exact analytical solutions: part i. Topology Optimization in Structural and Continuum Mechanics 549:1–14, doi:10.1007/978-3-7091-1643-2_1

Sadd MH (2005) Elasticity: theory, applications and numerics. Elsevier

Sigmund O, Aage N, Andreassen E (2016) On the (non-)optimality of Michell structures. Structural and Multidisciplinary Optimization doi:10.1007/s00158-016-1420-7

Sokół T, Rozvany GIN (2012) New analytical benchmarks for topology optimization and their implications. Structural and Multidisciplinary Optimization 46:477–486, doi:10.1007/s00158-012-0786-4

Spillers WR (1975) Iterative Structural Design. Elsevier

Strang G, Kohn R (1983) Hencky-Prandtl nets and constrained Michell trusses. Computer Methods in Applied Mechanics and Engineering 36:207–222, doi:10.1016/0045-7825(83)90113-5